Cleavage of the X−Pro Peptide Bond by Pepsin Is Specific for the *trans* Isomer†

Joseph E. Vance, Darryl A. LeBlanc, and Robert E. London*

Laboratory of Structural Biology, NIEHS, Box 12233, Research Triangle Park, North Carolina 27709

Received April 21, 1997; Revised Manuscript Received August 12, 1997⊗

ABSTRACT: Fluorine nuclear magnetic resonance studies of the cleavage of peptides containing a 4-fluorophenylalanine (FPhe)−Pro bond have been performed in order to determine the conformational specificity of FPhe−Pro bond cleavage by pepsin. The peptides selected were substrates of HIV protease or of avian sarcoma virus protease, both of which have been reported to be cleaved specifically at X−Pro by pepsin as well as by the corresponding viral protease enzyme. By working at 0 °C, it was possible to separate kinetically cleavage and *cis*/*trans* isomerization. For the case of the protease substrate, Ser-Gln-Asn-FPhe-Pro-Ile-Val-Gln, cleavage was shown to be specific for the *trans* conformation. A value for the rate constant for hydrolysis of the *trans* peptide divided by the Michaelis constant, $k_{tH}/K_M^{trans} = 0.3\ min^{-1}\ mM^{-1}$ was obtained with this substrate, and the Michaelis constant appears to be considerably higher than the substrate concentration, 3.7 mM, used in the study. On a slower time scale, additional cleavages can readily be detected. For the avian leukemia virus protease substrate, Thr-Phe-Gln-Ala-FPhe-Pro-Leu-Arg-Glu-Ala, the cleavage was both slower and less specific. In addition to the primary cleavage at the FPhe−Pro site, cleavage also occurs at the Ala-FPhe bond on a somewhat slower time scale. In addition to the conformational specificity of the cleavage reaction, these results indicate that pepsin is a better model for HIV protease than for avian leukemia virus protease.

Although cleavage of a tyrosyl−proline bond of ribonuclease A by pepsin was first noted by Huang and Tang in 1969, little subsequent work has been done on the characterization of imide bond proteolysis by this enzyme. Interest in the ability of pepsin to cleave peptidyl−proline bonds has been rekindled by the close structural analogy to viral aspartyl proteases (Miller et al., 1989). For example, both pepsin and HIV[1] protease are inhibited by pepstatin and its analogs (Seelmeier et al., 1988; Richards et al., 1989; Fitzgerald et al., 1990), and both possess the rare ability to cleave both amide and imide peptide bonds. Most reviews on pepsin do not discuss the activity of the enzyme on imide bonds, although there are several additional reports of such cleavage in the literature (Kottler et al., 1990; Copeland et al., 1990; Bedbeder et al., 1991). These are, to our knowledge, the only examples of cleavage of an imide proline bond by a mammalian aspartyl protease, the previous examples, prolidase, aminopeptidase P, and carboxypeptidase P, all being Mn^{2+}-dependent metalloproteases (Vanhoof et al., 1995), and in some cases, trypsin (Keil, 1992).

As pointed out initially by Lin and Brandts (1979a,b), one of the important features of such X−Pro cleavage is the conformational specificity of the reaction. We have recently demonstrated by fluorescence spectroscopy that cleavage of a fluorescent octapeptide containing a Tyr−Pro bond by HIV protease is selective for the *trans* isomer, so that a similar *trans* specificity of pepsin cleavage might be anticipated (Vance et al., 1997). Such a demonstration would, however, require extremely efficient cleavage of the peptide by pepsin, since the conformational specificity is only unmasked if the rate of enzymatic cleavage can be made much greater than the *cis*/*trans* isomerization rate. Furthermore, a recent study by Copeland et al. (1990) concluded that the Tyr−Pro bond of a peptide with sequence corresponding to the gag p17/p24 junction is not readily hydrolyzed by related pepsin-like aspartic proteinases, although a low activity was measured for pepsin itself. In the present study, we demonstrate the *trans* specificity of this cleavage reaction by pepsin using a fluorinated test peptide which is structurally analogous to the gag pl7/p24 junction cleaved by HIV protease.

MATERIALS AND METHODS

Sample and NMR Parameters

The *p*-fluorophenylalanine-containing peptides, [Ser-Gln-Asn-FPhe-Pro-Ile-Val-Gln] (FP-1), [Thr-Phe-Gln-Ala-FPhe-Pro-Leu-Arg-Glu-Ala] (FP-2), and [Ser-Gln-Asn-FPhe] (FP-3), were obtained from Macromolecular Resources, Inc. (Ft. Collins, CO). *p*-Fluoro-D,L-phenylalanine and other chemicals were obtained from Sigma (St. Louis, MO). Fluorinated peptides were used in these studies due to the high intrinsic detection sensitivity, spectral simplicity, and sensitivity of the shift to both *cis*/*trans* isomerism and proteolytic cleavage. All studies were performed using a 5 mm $^{19}F\{^1H\}$ probe on a Varian UnityPlus 500 (Varian Associates, Palo Alto, CA), operating at a ^{19}F NMR frequency of 470.996 MHz. Proton decoupling was accomplished with either a WALTZ (Shaka et al., 1983; applied throughout the magnetization transfer experiments) or a GARP (Shaka et al., 1985; applied during acquisition only for all other experiments) decoupling scheme. An extended-duration, high-stability temperature

† This work was supported by the NIEHS Intramural AIDS Research Program.

* Corresponding author.

⊗ Abstract published in *Advance ACS Abstracts,* October 1, 1997.

[1] Abbreviations: ASV, avian sarcoma virus; FP-1, fluorinated peptide 1, Ser-Gln-Asn-FPhe-Pro-Ile-Val-Gln; FP-2, fluorinated peptide 2, Thr-Phe-Gln-Ala-FPhe-Pro-Leu-Arg-Glu-Ala; FP-3, fluorinated peptide 3, Ser-Gln-Asn-FPhe; FPhe, L-4-fluorophenylalanine; NMR, nuclear magnetic resonance; HIV, human immunodeficiency virus; TFA, trifluoroacetate.

S0006-2960(97)00918-5

controller maintained temperature to ±0.1 °C. At high temperatures, the thermal equilibration of sample/probe was indicated by decreasing changes in probe tuning capacitance, linewidth, and chemical shift. The low temperature experiments used a rapid-mix injection system that allows observations of both reactants prior to mixing. Chemical shift referencing is to an external trifluoroacetate (TFA) standard.

Methods of Rapid Mixing

Kinetic studies of peptide hydrolysis and of *cis*/*trans* isomerization at low temperatures required the use of rapid-mixing techniques. The injection apparatus consists of a 10 cm glass insert open at both ends, connected by a 100 cm length of Tygon tubing to a 1 mL syringe located outside the magnet bore. The glass insert is submerged in the NMR tube to create coaxial cylindrical chambers, both of which are in the active region of the RF coil. The two ends of the insert are held in position by the curvature of the 5 mm NMR tube at the bottom and a Teflon bushing at the top. Typically, the mixing procedure involves injecting a small-volume, high-concentration component into a large-volume, low-concentration component. The principal experimental difficulty with the rapid-mixing approach is the large volume associated with the Tygon tubing which connects the concentric tube to the external syringe. In order to avoid filling the entire assembly with the concentrated peptide solution, a small volume of the solution is drawn into the glass insert, to a height approximately equal to that of the outer cylindrical chamber, which contains either buffer or enzyme solutions. To prevent uncontrolled mixing, a small barrier is created by drawing 1−2 mm of air and/or corn oil into the bottom of the insert prior to submersion into the larger volume component already present in the NMR tube. This approach allows shimming to be performed on the unmixed sample and NMR spectra to be acquired on a stable system prior to mixing. In the hydrolysis studies, typical parameters were 0.64 s acquisition time, 1.0 s delay, and 8 acquisitions/spectrum, resulting in 5 spectra stored per minute. Mixing is initiated by plunging the syringe to a predetermined depth and drawing it back to the initial position, and repeating this operation during the first 8-acquisition period.

Isomerization Rate Measurements

The *cis*/*trans* isomerization rates of the FPhe−Pro bond in FP-1 were measured using magnetization transfer methods at high temperature or, at lower temperatures, time-dependent spectroscopy of the peptide after dilution from a solvent with a different *cis*/*trans* ratio. The low-temperature measurements were based on the perturbed *cis*/*trans* ratios which have been observed in proline-containing peptides dissolved in LiCl/THF (Kofron et al., 1991). Via the injection apparatus discussed above, 75 μL of a concentrated (65−75 mM) solution of the fluorinated peptide FP-1 in 0.4 M LiCl/THF was initially placed in the concentric capillary. After obtaining premix ^{19}F spectra which corresponded to a *cis*/*trans* ratio of ∼0.6, the peptide was rapidly added to 530 μL of 1 M NaCl, 50 mM deuteroacetate (pH 5.0), 100% D_2O buffer, yielding a postmix peptide concentration of 9−10 mM. As described below, the isomerization rate was determined from the time-dependent intensities of the *cis* and *trans* resonances as they approached an equilibrium ratio of ∼0.35, characteristic of the peptide in aqueous solution. Macros written for the Varian UnityPlus spectrometer allowed for postprocessing whereby specified spectra are selected and averaged to provide an adjustable balance between the signal to noise ratio (SNR) and temporal resolution.

The simple imide bond isomerization process can be described by the equations

$$\frac{\mathrm{d[Trans]}}{\mathrm{d}t} = -k_t[\mathrm{Trans}] + k_c[\mathrm{Cis}]$$

$$\frac{\mathrm{d[Cis]}}{\mathrm{d}t} = -k_c[\mathrm{Cis}] + k_t[\mathrm{Trans}] \qquad (1)$$

where k_c and k_t are rate constants for *cis*→*trans* and *trans*→*cis* interconversion, respectively. Solution of these equations subject to the initial conditions, $\mathrm{Cis}[0] = \mathrm{Cis_i}$; $\mathrm{Trans}[0] = \mathrm{Trans_i}$, gives the result

$$\mathrm{Cis}[t] = \mathrm{Cis_e} + (\mathrm{Cis_i} - \mathrm{Cis_e})\mathrm{e}^{-(k_c+k_t)t}$$

$$= \mathrm{Cis_e} + (\mathrm{Cis_i} - \mathrm{Cis_e})\mathrm{e}^{-(k_c/\mathrm{Trans_e})t}$$

$$\mathrm{Trans}[t] = \mathrm{Trans_e} + (\mathrm{Trans_i} - \mathrm{Trans_e})\mathrm{e}^{-(k_c+k_t)t}$$

$$= \mathrm{Trans_e} + (\mathrm{Trans_i} - \mathrm{Trans_e})\mathrm{e}^{-(k_c/\mathrm{Trans_e})t} \qquad (2)$$

where the subscripts indicate initial or equilibrium populations. Regression of time series data subject to initial (perturbed) and final (equilibrium) boundary conditions yields k_c and k_t at low temperatures.

At higher temperatures, isomerization and relaxation rates are comparable, yielding signal intensities no longer simply related to conformer populations. However, isomerization rate constants are distinguishable from relaxation rates at temperatures of 50−80 °C using magnetization transfer methods analogous to those used previously in studies of fluorinated bradykinin analogs (London et al., 1990). A DANTE pulse train (Morris & Freeman, 1978) is used to selectively invert either the *trans* or the *cis* fluorine resonances of the peptide, followed by a nonselective 90° read pulse after delays of 1×10^{-5}, 0.1, 0.2, 0.3, 0.4, 0.5, 0.6, 0.7, 0.8, 0.9, 1.0, and 15 s. Data analysis follows the method described by Perrin and Engler (1990) in which peak intensities from both the *cis* and *trans* inversion experiments at each mixing time, t_m, are organized into a series of 2 × 2 matrices, $\mathbf{M}(t_m)$, and diagonalized, and the resulting elements are fit to a linear function of time:

$$\ln[(\mathbf{M} - \mathbf{M}_{eq})\cdot(\mathbf{M}_o - \mathbf{M}_{eq})^{-1}] = \mathbf{X}\,(\ln \mathbf{\Lambda})\mathbf{X}^{-1} = -t_m\mathbf{R} \qquad (3)$$

$\mathbf{M}_o$ corresponds to the data matrix at $t_m = 0$, $\mathbf{M}_{eq}$ corresponds to the matrix of the fully relaxed system, and $\mathbf{X}$ is a square matrix of eigenvectors that transforms $[(\mathbf{M} - \mathbf{M}_{eq})\cdot(\mathbf{M}_o - \mathbf{M}_{eq})^{-1}]$ into the diagonal matrix $\mathbf{\Lambda}$. A linear least squares fit of the data yields the elements of the relaxation matrix

$$\begin{bmatrix} R_{11} & R_{12} \\ R_{21} & R_{22} \end{bmatrix} = \begin{bmatrix} \frac{1}{T_{1c}} + k_c & -k_t \\ -k_c & \frac{1}{T_{1t}} + k_t \end{bmatrix} \qquad (4)$$

where k_c and k_t are defined by eq 1 above and T_{1c} and T_{1t} are the spin−lattice relaxation time constants for the *cis* and *trans* species, respectively.

Data Analysis

Analysis of the isomerization rate data and the pepsin hydrolysis data was accomplished using a series of programs written in Mathematica (Version 2.2, Wolfram Research, Urbana, IL). For the magnetization transfer studies, the program diagonalizes a series of 2 × 2 data matrices and performs a linear fit for each matrix element, as described above. For the lower temperature dilution/isomerization studies and for the pepsin hydrolysis studies using the analytical formalism given above, data were fit using the nonlinear least squares routine available in Mathematica. For the more complex kinetic schemes, the set of differential equations was solved numerically using the DSolve routine in Mathematica, subject to the appropriate set of initial conditions.

For the kinetic studies, the sum of the resonance intensities of the *cis*, *trans*, and product peaks was normalized to 1, prior to fitting. In some cases (e.g., Figure 5A), some premixing of the pepsin with the peptide occurred, leading to the observation of small product resonance(s). The intensity of these product resonances, formed prior to initiation of the kinetic study, was subtracted from the observed product resonance in each subsequent spectrum.

THEORETICAL ANALYSIS

A general kinetic scheme for the hydrolysis of a peptide exhibiting slow *cis*/*trans* interconversion kinetics is illustrated in Kinetic Model I (Scheme 1), where k_t and k_c describe the

Scheme 1

Kinetic Model I

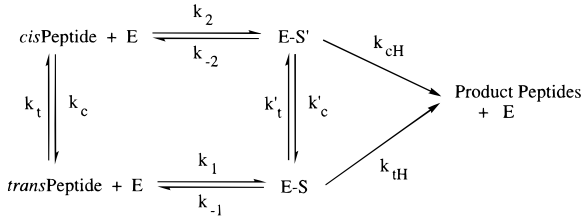

interconversion rates for the free peptide, related by $f_{cis}k_c = f_{trans}k_t$, f_{cis} and f_{trans} are the fractional *cis* and *trans* equilibrium concentrations, k_t' and k_c' are the corresponding interconversion rates of the enzyme-complexed peptide, k_1, k_{-1}, k_2, and k_{-2} are the rate constants for binding and dissociation of the *trans* and *cis* peptides to the enzyme, and k_{cH} and k_{tH} are the hydrolysis rates of the *cis* and *trans* enzyme complexes. In setting up this analysis, we have followed the standard approach of representing hydrolysis as irreversible, although in fact, the equilibrium relating the unhydrolyzed to hydrolyzed peptides is just far toward complete hydrolysis. A set of differential equations corresponding to the above kinetic scheme can be written and solved numerically subject to a set of initial conditions using the program Mathematica. Typical initial conditions used are Cis[0] = Cis_e, Trans[0] = Trans_e, and enzyme−substrate complexes at time zero, E−S[0] = 0, where the subscript e indicates the equilibrium value. Although data can be fit using this approach, it is in general not possible to obtain unique solutions for the large number of parameters involved.

Scheme 2

Kinetic Model II

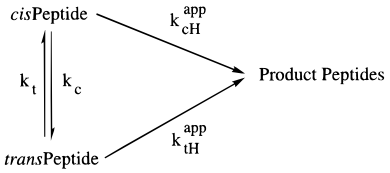

Alternatively, a simplified kinetic model was also used (Scheme 2). This model can be solved analytically and thus provides a useful algorithm for a nonlinear least squares fit of the data using a limited parameter set. In the Michaelis limit of Model I in which the rate constants k_1, k_{-1}, k_2, and k_{-2} are much larger than any of the other rate constants which enter the problem, such that the uncomplexed and enzyme-complexed substrates are in effective equilibrium, the Michaelis constants are given by

$$K_M^{trans} = \frac{k_{-1} + k_{tH}}{k_1} \approx \frac{k_{-1}}{k_1}$$

$$K_M^{cis} = \frac{k_{-2} + k_{cH}}{k_2} \approx \frac{k_{-2}}{k_2} \qquad (5)$$

In this limit, the analytical solutions of Kinetic Model II become very good approximations to the behavior of Model I as long as the total substrate concentration $S_o \ll K_M^{cis}, K_M^{trans}$. In this case, the apparent hydrolysis rate constant which enters kinetic model II is given by

$$k_{tH}^{app}\ (\text{Model II}) = k_{tH}\ (\text{Model I})\frac{E_o}{S_o + K_M^{trans}} \approx k_{tH}\frac{E_o}{K_M^{trans}} \qquad (6)$$

A similar relation exists for $k_{cH}{}^{app}$ and k_{cH}. Although the differential equations become non-first-order as S_o approaches K_M, the use of Model II is found empirically to give a better approximation to Model I by keeping the S_o term in the denominator above as long as $S_o < K_M$. The solution to Kinetic Model II can be obtained from the set of coupled differential equations given below

$$\frac{d[\text{Trans}]}{dt} = -(k_t + k_{tH})[\text{Trans}] + k_c[\text{Cis}]$$

$$\frac{d[\text{Cis}]}{dt} = -(k_c + k_{cH})[\text{Cis}] + k_t[\text{Trans}] \qquad (7)$$

$$\frac{d[\text{Prod}]}{dt} = k_{tH}[\text{Trans}] + k_{cH}[\text{Cis}]$$

where the last equation is equivalent to a normalization condition. In the above equations and in the constants given below, we have omitted the "app" superscript for simplicity, and in the discussion below, this is only included when making a distinction between Model I and Model II parameters. These equations can be solved analytically, subject to the following initial conditions: Cis[0] = Cis_e = $k_t/(k_c + k_t)$, Trans[0] = Trans_e = $k_c/(k_c + k_t)$, and Prod[0] = 0. The time dependent Cis, Trans, and Prod (either product

peptide) concentrations are described as a sum of two exponential terms according to

$$\mathrm{Cis}[t] = (\mathrm{Cis_e}\, C_1 - \mathrm{Trans_e}\, C_3)e^{-\lambda_1 t} + (\mathrm{Cis_e}\, C_2 + \mathrm{Trans_e}\, C_3)e^{-\lambda_2 t}$$

$$\mathrm{Trans}[t] = (\mathrm{Trans_e}\, C_2 - \mathrm{Cis_e}\, C_4)e^{-\lambda_1 t} + (\mathrm{Trans_e}\, C_1 + \mathrm{Cis_e}\, C_4)e^{-\lambda_2 t}$$

$$\begin{aligned}\mathrm{Prod}[t] &= 1 - \mathrm{Cis}[t] - \mathrm{Trans}[t] \\ &= 1 - (\mathrm{Cis_e}\, C_1 - \mathrm{Trans_e}\, C_3 + \mathrm{Trans_e}\, C_2 - \mathrm{Cis_e}\, C_4)e^{-\lambda_1 t} - (\mathrm{Cis_e}\, C_2 + \mathrm{Trans_e}\, C_3 + \mathrm{Trans_e}\, C_1 + \mathrm{Cis_e}\, C_4)e^{-\lambda_2 t} \quad (8)\end{aligned}$$

where the time constants λ_1 and λ_2 are given by

$$\lambda_1 = {}^1/_2(k_c + k_t + k_{cH} + k_{tH} + R_1)$$

$$\lambda_2 = {}^1/_2(k_c + k_t + k_{cH} + k_{tH} - R_1) \quad (9)$$

where R_1 is given by

$$R_1 = \begin{pmatrix} k_c^2 + k_t^2 + k_{cH}^2 + k_{tH}^2 + 2k_c k_t - 2k_{cH}k_{tH} \\ -2k_c k_{tH} - 2k_t k_{cH} + 2k_c k_{cH} + 2k_t k_{tH} \end{pmatrix}^{1/2} \quad (10)$$

and the constants C_i are given by

$$C_1 = \frac{k_c + k_{cH} - k_t - k_{tH} + R_1}{2R_1}$$

$$C_2 = \frac{k_t + k_{tH} - k_c - k_{cH} + R_1}{2R_1}$$

$$C_3 = \frac{k_t}{R_1}$$

$$C_4 = \frac{k_c}{R_1} \quad (11)$$

Experimental resonance intensities for the *cis* and *trans* isomers of the substrate peptide and for the product peptide can then be analyzed using the above relations. Equations 8−11 demonstrate that, analogous to earlier treatments of conformational dependent cleavage (Lin & Brandts, 1979), the product formation can be described as a sum of two exponentials with time constants λ_1 and λ_2. In the limit $k_{tH} \gg k_c$, $\lambda_1 \rightarrow k_{tH}$ and $\lambda_2 \rightarrow k_c$ for $k_{cH} = 0$. In kinetic studies using other spectroscopic methods, only the product (or precursor) concentration is determined as a function of time. As outlined above, this concentration will in general exhibit biexponential kinetics according to

$$\mathrm{Prod}[t] = 1 - \mathrm{Coef_1}\, e^{-\lambda_1 t} - \mathrm{Coef_2}\, e^{-\lambda_2 t} \quad (12)$$

where explicit values for $\mathrm{Coef_1}$ and $\mathrm{Coef_2}$ are obtained using eqs 8 and 11.

The Trans[t]/Cis[t] ratio provides a sensitive indication of the relative hydrolysis rates of the *cis* or *trans* peptide conformations. The ratio drops from the initial equilibrium value to a limiting value which is dependent on k_{cH} and k_{tH}.

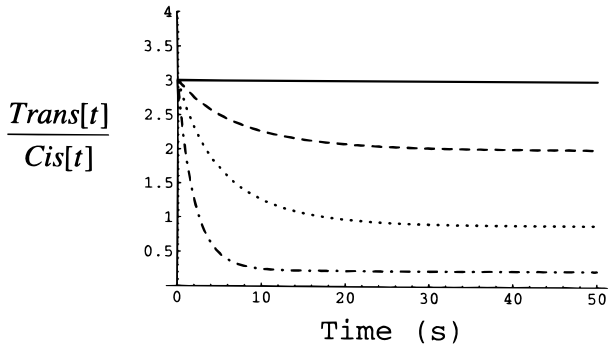

FIGURE 1: Theoretical kinetic behavior of the *trans*/*cis* ratio as a function of time using parameters $\mathrm{Trans_e}/\mathrm{Cis_e} = 3.0$, $k_c = 0.1\ s^{-1}$, $k_{tH} = 0.5\ s^{-1}$, and $k_{cH}/k_{tH} = 1.0$ (—), 0.9 (- - -), 0.7 (···), or 0 (—·—).

If $k_{tH} = k_{cH}$, the ratio remains unchanged, whereas if $k_{tH} > k_{cH}$, the ratio drops to a limiting value:

$$\mathrm{Lim}\left[\frac{\mathrm{Trans}[t]}{\mathrm{Cis}[t]}\right]_{t\rightarrow\infty} = \frac{\mathrm{Cis_e}\, C_4 + \mathrm{Trans_e}\, C_1}{\mathrm{Cis_e}\, C_2 + \mathrm{Trans_e}\, C_3} \quad (13)$$

The behavior of Trans[t]/Cis[t] as a function of time for various values of the ratio k_{cH}/k_{tH} is shown in Figure 1. A change in the Trans/Cis ratio from its equilibrium value is indicative of conformational selectivity of cleavage. Although this behavior is strongly characteristic of the relative hydrolysis rates of the two conformations, this type of analysis has some practical limitations since at long times the intensities of the substrate *cis* and *trans* resonances become extremely small and subject to large errors. Furthermore, different models, including the inclusion of subsequent proteolytic cleavage of the product peptides, or the inclusion of reversibility, significantly alter the limiting value of the ratio. For example, if $k_{cH} = 0$ and a small rate constant for peptide resynthesis is included in eq 4, the Trans/Cis ratio drops initially, but ultimately recovers to its initial, equilibrium value. Nevertheless, the initial change in this ratio can be highly informative. Further, the analysis given above is useful for situations that deviate significantly from the limit $k_{tH} \gg k_c$, which can be the case when bonds located near proline residues, rather than the X−Pro bonds themselves, are cleaved (Fischer et al., 1984; Lin & Brandts, 1985). The most sensitive constraint on k_{cH} arises from the time dependence of the *cis* isomer concentration. If k_{cH} approaches k_c, then the *cis* isomer concentration decays more rapidly, and this ultimately puts the lowest upper limit on the value of k_{cH}. Hence, the strongest limit on k_{cH} can be determined under conditions corresponding to the lowest value of k_c.

RESULTS

Isomerization Rates

As discussed above and elsewhere (Vance et al., 1997), the fluorine NMR spectrum of the fluorinated octapeptide substrate FP-1 exhibits two ^{19}F resonances 0.6 ppm apart, at a ratio equal to the *cis*/*trans* ratios for the other nuclear resonances of the peptide (^{13}C, ^1H). Magnetization transfer studies of FP-1 performed at temperatures >40 °C, analogous to our previous studies with 4-fluorophenylalanine-substituted bradykinin (London et al., 1990), demonstrate that the two resonances correspond to a single, interconverting species.

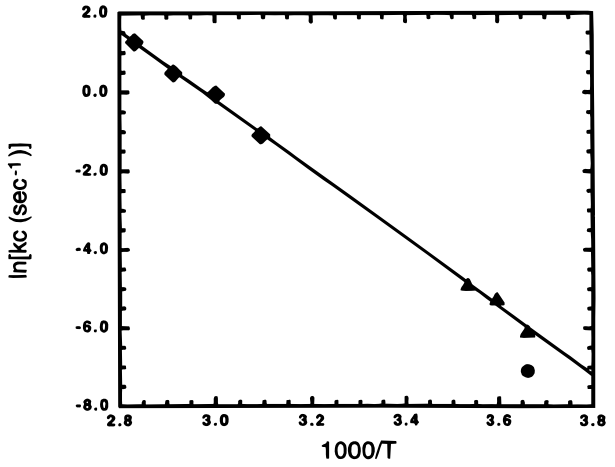

FIGURE 2: The *cis* → *trans* isomerization rate constant, k_c, plotted as a function of 1000/*T* for FP-1. The higher temperature data (◆) were obtained using magnetization transfer techniques on a sample of 3.7 mM FP-1 in 1 M NaCl, 50 mM deuteroacetate, pH 5.0, and 100% D_2O. Lower temperature data (▲) were obtained by solvent/dilution methods where the intensities of the *cis* and *trans* resonances are monitored by NMR following the rapid injection of a 75 μL solution of 65−75 mM FP-1 in 0.4 M LiCl in TFE to 530 μL of 1 M NaCl, 50 mM deuteroacetate, pH 5.0, and 100% D_2O buffer solution. The linear fit corresponds to the activation energy $\Delta G = 17.4$ kcal/mol. The value of k_c obtained at 0 °C based on the analysis of the hydrolysis of FP-1 is also shown (●).

A plot of the *cis*→*trans* rate constant, k_c, as a function of temperature is shown in Figure 2. Interconversion rates at lower temperature were measured on the basis of peptide dilution from a 0.4 M LiCl/TFE solvent into a 1 M NaCl, 50 mM deuteroacetate (pH 5.0) solution, as described in Materials and Methods. The results of experiments at 0, 5, and 10 °C are seen in Figure 2 to be consistent with those obtained from high temperature magnetization transfer studies. A fit of the temperature dependent rate constant k_c to an Arrhenius relation of the form $k_c = k_o e^{-\Delta G/RT}$, where $R = 1.987 \times 10^{-3}$ kcal/K·mol, yielded an isomerization free energy $\Delta G = 17.4$ kcal mol^{-1}. This value is consistent with reported values for other proline-containing peptides (Stein, 1993).

Hydrolysis Kinetics of FP-1

In the presence of 0.5 mM pepsin, FP-1 is initially hydrolyzed to give a product with a single resonance at −40.92 ppm (P1, Figure 3). Over a longer time scale (hours), two additional resonances are observed at −40.97 ppm (P2) and −39.80 ppm. On the basis of previous studies with the related peptide, Val-Ser-Gln-Asn-Tyr-Pro-Ile-Val-Gln-NH_2 (Copeland et al., 1990) and of the appearance of a single product resonance indicating the absence of a *cis*/*trans* equilibrium, initial cleavage occurs at the FPhe−Pro bond, producing two product tetrapeptides. Since pepsin is a digestive enzyme, it is not surprising that additional cleavages occur. Spiking the sample with the tetrapeptide Ser-Gln-Asn-FPhe or with 4-fluoro-D,L-phenylalanine allowed unequivocal assignment of the initially formed product to the former and of the final observed product to the latter. The second product, P2, with a resonance close to that of the tetrapeptide presumably corresponds either to Asn-FPhe or to Gln-Asn-FPhe. Since this product lacks resonances corresponding to *cis* and *trans* isomers, it is presumably

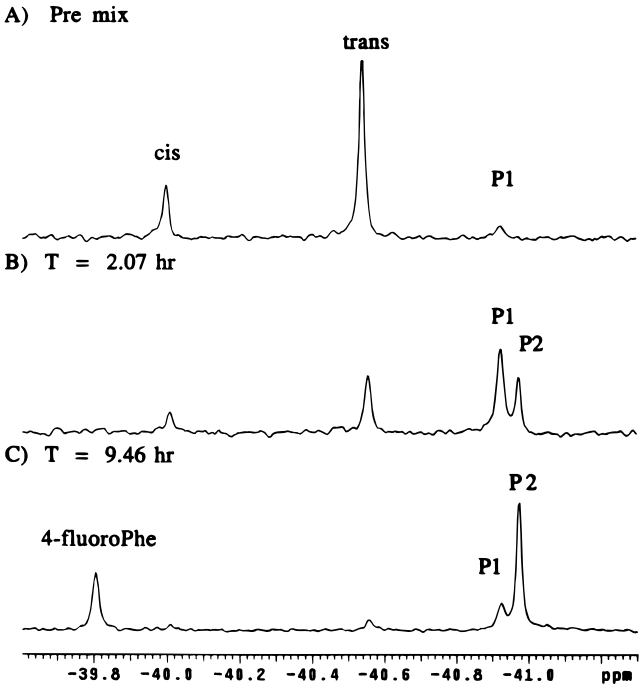

FIGURE 3: Proton decoupled ^{19}F NMR spectra of FP-1 (3.7 mM). (A) Premix spectrum showing *cis* and *trans* isomers of the peptide FP-1 which is present in the capillary, as described in Materials and Methods. Note that, although mixing had not been initiated, a small product resonance, not seen in the pure material, is observable, which arises due to some premixing of the peptide substrate with the pepsin. This limited amount of product is created during sample assembly, and a simple correction is made in the kinetic analysis. (B) Spectrum after 2.07 h of exposure to 0.5 mM pepsin in 1 M NaCl, 0.1 M citrate, pH 4.0, and 20% D_2O. (C) ^{19}F NMR spectrum after 9.46 h of exposure. The major initial product observed, P1, corresponds to the tetrapeptide, Ser-Gln-Asn-FPhe, as demonstrated, for example, by the addition of the known peptide. The unidentified product with a resonance close to that of the tetrapeptide, P2, corresponds to a subsequent hydrolysis product, either Gln-Asn-FPhe or Asn-FPhe. After long periods of time, a ^{19}F resonance corresponding to free FPhe is also observed at −39.8 ppm.

formed as a result of subsequent hydrolysis of the tetrapeptide Ser-Gln-Asn-FPhe.

In order to kinetically separate the peptide cleavage and conformational isomerization processes, it is necessary to increase the rate of the former and to reduce the rate of the latter. Although some of the initial kinetic studies were performed in 100% D_2O, most of the studies were performed in 20% D_2O. The use of a lower deuteration level was suggested by previous studies indicating that peak hydrolysis rates are considerably higher in H_2O than in D_2O (Hunkapiller & Richards, 1972). High salt is also reported to increase the activity of both pepsin and the proteases (Kotler et al., 1989; Wondrak et al., 1991; Meek et al., 1994), and studies were performed in 1 M NaCl. A series of time-dependent $^{19}F\{^1H\}$ spectra of the peptide FP-1 subsequent to addition to the buffered pepsin solution is shown in Figure 4. These spectra, obtained at 0 °C with 3.7 mM peptide (postmix) and a pepsin concentration of 2 mM, show the characteristic rapid decline of the *trans* species and decrease in the *trans*/*cis* ratio to values <1.0, as predicted theoretically, e.g., in Figure 1. By the fifth time period, [Trans] < [Cis], and by the sixteenth time period, the ^{19}F resonance of the *trans* species is barely visible. In these studies, no product at the P2 resonance position was observed, as seen with 0.5 mM pepsin (Figure 3), due to the somewhat broader linewidths

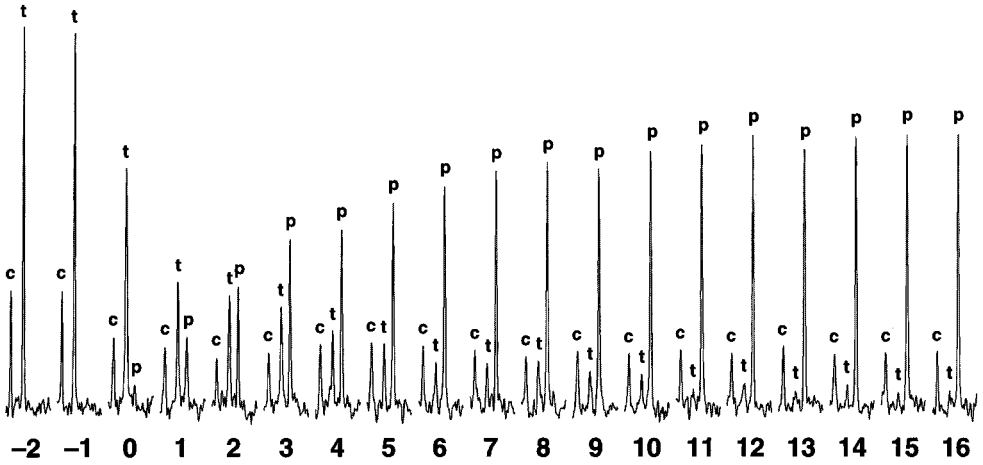

FIGURE 4: Time dependent ^{19}F NMR spectra obtained at 0 °C prior to injection (−2,−1), during injection (0), and after addition (+1,16) of FP-1 (final concentration = 3.7 mM) to a sample containing 2 mM pepsin in 1 M NaCl, 0.1 M citrate, pH 4.0, and 20% D_2O. Alternate blocks of spectra corresponding to 8 scans each, with a time resolution of 26.24 s, are shown, so that the 16 spectra in the figure correspond to the first seven minutes after mixing. Observed ^{19}F resonances correspond to the FP-1 *cis* (c) and *trans* (t) conformations and to the product peptides (p). The latter arise primarily from the tetrapeptide Ser-Gln-Asn-FPhe, as well as from products other than free FPhe, which is formed on a considerably slower time scale and resonates further downfield (Figure 3).

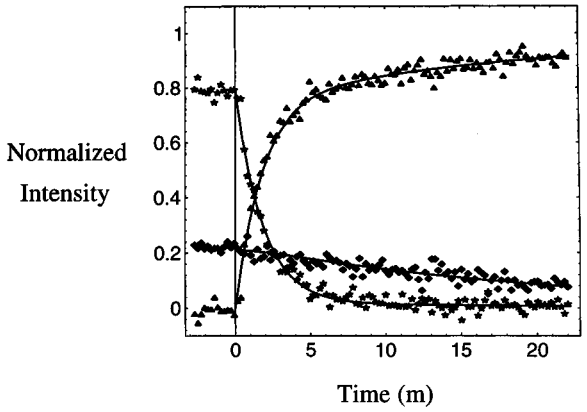

FIGURE 5: Kinetic data plotted as normalized intensity against time (min), derived from the spectra of Figure 4 and analyzed using numerical solutions of Kinetic Model II. Data correspond to the FP-1 *trans* concentration (★), FP-1 *cis* concentration (◆), and product concentration (▲). The spectral peak heights are normalized as described in Materials and Methods. Average normalized intensities at 0 °C prior to mixing ($t < 0$) give fractional populations of 0.21 for Cis and 0.79 for Trans or Cis/Trans = 0.27. A short burst phase due to a temporary elevation of S_o during injection was found to create 5% of the final product and was removed to first-order by an overall 5% reduction (prior to normalization) of product for $t > 0$. The solid line is the numerical best fit of Kinetic Model II to the data using the parameters $k_c = 0.048$ min^{-1}, $k_{tH}^{app} = 0.56$ min^{-1}, with $\chi^2 = 0.065$.

at the higher enzyme concentration, and to the fact that the ^{19}F resonance of P1 is shifted further upfield, presumably due to an exchange-averaged shift involving free and pepsin-associated peptide.

Initially, the ^{19}F NMR hydrolysis data (Figure 5) were fit using the analytical expression for the product concentration derived from Kinetic Model II above (eq 8) and the nonlinear least squares capability of Mathematica, Version 2.2. A two-parameter fit with k_c and k_{tH}^{app} as variables yielded $k_c = 0.048$ min^{-1}, $k_{tH}^{app} = 0.56$ min^{-1}, with $\chi^2 = 0.065$. If k_{cH}^{app} was also allowed to vary, the optimal fit yielded $k_c = 0.051$ min^{-1}, $k_{tH}^{app} = 0.56$ min^{-1}, and $k_{cH}^{app} = -0.002$ min^{-1}, with $\chi^2 = 0.065$. Hence, allowing k_{cH}^{app} to vary does not produce a significant improvement in the data fit, and leads to very small, and in this case negative, values for k_{cH}^{app}. The use of Kinetic Model I in its full or simplified version involves a larger number of variable parameters. Assuming, consistent with the fit to Model II, that the *cis* form of the peptide does not bind to the enzyme, numerical simulation of the kinetic curves indicates that optimal parameters correspond to high values of the Michaelis constant K_M. For example, a close simulation of the experimental data shown in Figure 5 may be obtained using the parameters $k_c = 0.05$ min^{-1}, $k_t = 0.013$ min^{-1}, $k_1 = 3 \times 10^4$ min^{-1} mM^{-1}, $k_{-1} = 90 \times 10^4$ min^{-1} (corresponding to $K_M^{trans} = 30$ mM), $k_{tH} = 9.1$ min^{-1}, and $k_{cH} = 0$. As discussed above, this fit would correspond to an apparent *trans* hydrolysis rate constant $k_{tH}^{app} \sim k_{tH}(E_o/K_M^{trans}) = 0.61$ min^{-1}, in good agreement with the value of 0.56 min^{-1} obtained directly by fitting the data to the analytical expression in Model II. Taken together, these analyses indicate that the K_M^{trans} value for the interaction of FP-1 with pepsin is fairly large and that it is only possible to extract the ratio $k_{tH}/K_M^{trans} = 0.28$ min^{-1} mM^{-1} from these studies. A large K_M^{trans} value is also not unreasonable, given the fact that millimolar K_M values have been reported for the interaction of similar peptides with HIV protease. For example, Darke et al. (1989) report $K_M = 1.5$ mM for the corresponding FPhe→Tyr peptide, Ser-Gln-Asn-Tyr-Pro-Ile-Val-Gln. Millimolar K_M values for HIV protease cleavage of other closely related peptides have also been reported (Tomasselli et al., 1990; Moore et al., 1989). In addition, the comparative activities of pepsin and HIV protease on the related test peptide, Val-Ser-Gln-Asn-Tyr-Pro-Ile-Val-Gln-NH_2 (Copeland et al., 1990), are consistent with a considerably higher K_M value for the former enzyme.

A plot of Trans[*t*]/Cis[*t*] for the same data (Figure 6) shows the characteristic decline predicted theoretically in Figure 1 for the case of $k_{cH} = 0$. Surprisingly, the value of k_c obtained in three independent studies was somewhat lower than the value predicted for $T = 0$ °C (Figure 2). It is unclear why this should be the case; indeed, it is conceivable that pepsin could possess some peptidyl−proline isomerase activity, as indicated in Kinetic Model I. Apparently this is not the case; the presence of the enzyme appears to retard the isomerization reaction to a small extent. It must be concluded that the rate of hydrolysis of the *cis* isomer, should it occur at all, is much slower than k_c, i.e., $k_{cH}^{app} \ll k_c$. On the basis

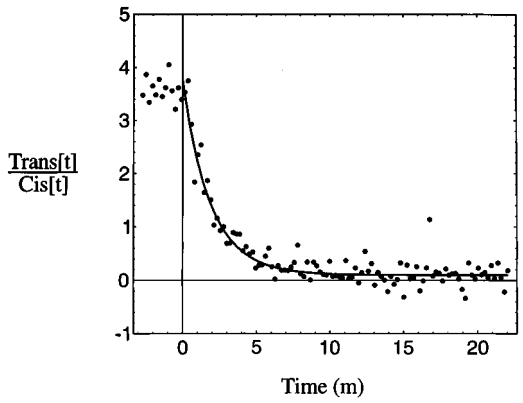

FIGURE 6: Kinetic data showing the experimental and theoretical Trans/Cis ratio as a function of time (in min) after mixing ($t = 0$). Experimental data are derived from Figure 4 and the theoretical curve is obtained using the parameters given in Figure 5. Models with k_c other than zero show significant deviations from the data and establish an upper limit for *cis* hydrolysis of $k_{cH}^{app}/k_{tH}^{app} < 0.01$.

of the data analysis given above, hydrolysis of the *cis* isomer is at least 2 orders of magnitude slower than k_{tH}^{app}. Studies (not shown) in which different enzyme concentrations were used show the expected variation in k_{tH}, with the slow time constant for disappearance of the *cis* isomer essentially unchanged.

Hydrolysis Kinetics of FP-2

Kotler et al. (1989) have shown that the decapeptide, Thr-Phe-Gln-Ala-Phe-Pro-Leu-Arg-Glu-Ala, which is one of the target peptides for the aspartyl protease from avian sarcoma virus, is also a substrate for pepsin and is selectively cleaved at the Phe−Pro bond. We therefore also studied the cleavage of the corresponding Phe→FPhe peptide (FP-2) using ^{19}F NMR (Figure 7). Under the conditions of the NMR studies, hydrolysis of FP-2 was found to be too slow to allow observation of significant differences in the *cis*/*trans* ratio, as was possible in the studies of FP-1. In addition to the product resonances which exhibit ^{19}F shifts close to those seen in the FP-1 study, one of the product peaks (P3) was strongly shifted downfield. Some free FPhe is also observed to form at longer times (Figure 7).

Effects of Terminal Amino and Carboxyl Groups on the ^{19}F Shift

Since the formation of N- or C-terminal FPhe can significantly perturb the chemical shift, we performed a pH titration study of FPhe (Figure 8). The p*K* values obtained, 2.62 and 9.26, are in excellent agreement with the values of 2.58 and 9.24 reported for phenylalanine (*Merck Index*, 8th ed.). Deprotonation of the carboxyl group produces an upfield shift of 0.57 ppm, while protonation of the amino group produces a downfield shift of 1.72 ppm. Hence, these shifts are consistent with the conclusion that the products showing up at higher field correspond to peptides with C-terminal FPhe, while product P3, which is shifted downfield of the *trans* resonance of FP-2 by ~1.6 ppm, corresponds to a product peptide with an N-terminal FPhe. The observation of this resonance indicates that, although the FPhe−Pro bond is the primary cleavage site on the peptide, some of the initial cleavage occurs at the Ala−FPhe bond. Additionally, if this is the case, then the FPhe-Pro-Leu-Arg-Glu-Ala product which is produced would still have an intact FPhe−Pro bond and hence would also be expected to exhibit *cis*/*trans* isomerism. In fact, longer averaging of the ^{19}F spectra shows a small resonance which is 0.6 ppm downfield of the P3 resonance shown in Figure 7. Hence, we interpret P3 and the downfield resonance as corresponding to the *trans* and *cis* resonances of FPhe-Pro-Leu-Arg-Glu-Ala.

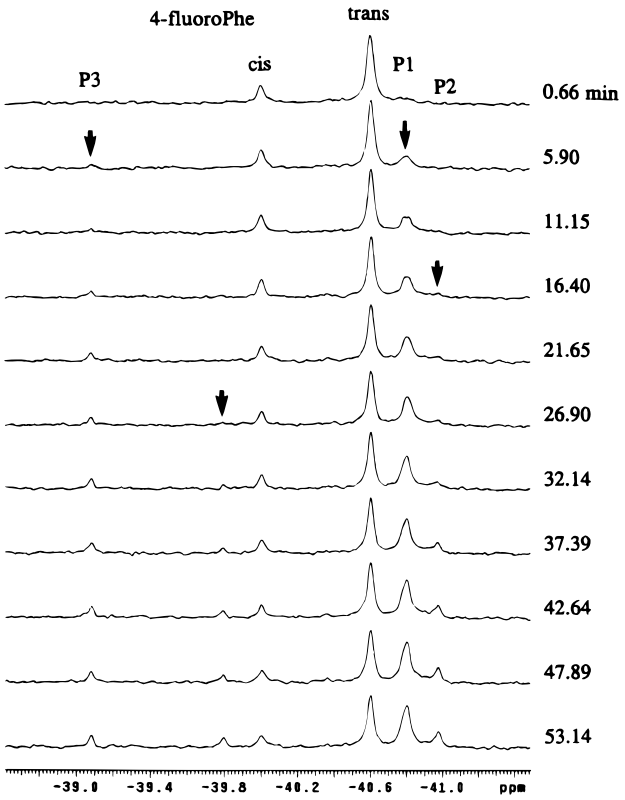

FIGURE 7: Time dependent ^{19}F NMR spectra obtained at 0 °C after addition of 70 μL of 50 mM FP-2 peptide to a 530 μL sample containing 1.5 mM pepsin in 1 M NaCl, 0.1 M citrate, pH 4.0, and 20% D_2O. Each spectrum represents an average over 1.32 min, and every fourth spectrum is shown, with the total time course corresponding to the first hour after mixing. In spectra obtained 12 h later (not shown), an additional peak appears at −38.4 ppm which is assigned to the *cis* isomer of P3.

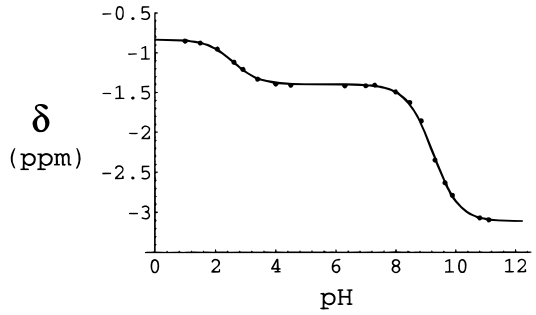

FIGURE 8: ^{19}F shift vs pH for FPhe at 25 °C. Sample contained 30 mM 4-fluoro-D,L-phenylalanine in 1 M NaCl, and 5 mM *o*-fluorobenzamide as an internal shift standard.

CONCLUSIONS

Proteases capable of hydrolyzing imide bonds in proline-containing peptides are fairly rare. Although the ability of pepsin to cleave X−Pro bonds was initially recognized in 1969 (Huang & Tang), there has been little further characterization of this cleavage, and no information was available on the conformational selectivity of the enzyme-catalyzed

reaction. Although conformational information can be derived using any method of product or substrate quantitation under conditions in which the peptide hydrolysis rate is rapid compared with the imide bond isomerization rate, the observation of complex kinetics can sometimes have other origins, making the interpretation less straightforward. Kinetic evaluations based on NMR measurements offer the unique ability to quantitate not only the product concentration but also the concentrations of the *cis* and *trans* forms of the substrate peptide. This approach has been utilized previously in studies of the hydrolysis of Ala−Pro by prolidase (King et al., 1986). However, the problem studied here involving cleavage of the X−Pro bond in a longer peptide is somewhat more challenging due to the much higher rate of isomerization. Such studies require kinetic measurements at temperatures close to 0 °C.

In order to analyze the kinetics of conformationally dependent enzyme cleavage, previous workers have used several approaches: (1) assumptions of cleavage and isomerization rate constants so different that k_{tH} and k_c values can be obtained directly from the kinetic data; (2) numerical solutions of differential equations modeling the process (King et al., 1986); (3) "initial rate" measurements which in fact ignore the initial hydrolysis "burst" corresponding to the *trans* peptide, and monitor the slower subsequent hydrolysis rate (Kofron et al., 1991). All of these approaches have some important limitations. In the case of pepsin, the hydrolysis of the test peptides studied proceeds slowly enough so that an ideal kinetic separation cannot be achieved. This situation completely eliminates the "initial rate" approach as a viable method for deriving kinetic information. Another limitation occurs if the hydrolysis is not completely conformationally specific. The numerical solution approach, which has been used in some of the analyses given here, is useful but time-consuming, particularly if several of the parameters are to be optimized.

The simplified set of equations presented here, valid in the limit $S_o \ll K_M$, provide an attractive approach for the analysis of conformationally dependent protease kinetics. In this limit, biexponential behavior is predicted and the data are fit to obtain kinetic parameters. Information on K_M can also be obtained, if S_o concentrations approaching the K_M value are used. No assumptions need to be made regarding the relative rates of hydrolysis of *cis* and *trans* precursors, and no initial rate approximations, which as noted above are often of limited value for this type of analysis, need to be invoked. Although cleavage of X−Pro by pepsin probably does exhibit a very high degree of isomeric selectivity, the cleavage of amide peptide bonds which are located near proline would generally be expected to have a lower selectivity for a particular isomeric state of the X−Pro bond. Several examples have been discussed in the literature (Fischer et al., 1984; Lin & Brandts, 1985). In contrast with the numerical methods noted above, rapid solution of the analytical expressions is useful for quantitatively fitting data using nonlinear least squares programs.

Both analytical and numerical analyses of the data indicate a high degree of selectivity of pepsin cleavage for the *trans* peptide isomer. As discussed above, k_{cH}^{app} must be at least 2 orders of magnitude lower than k_{tH}^{app} for cleavage of FP-1. Indeed, analysis of the data with a three-parameter fit using Kinetic Model II gave small, negative values for k_{cH}^{app}. In general, the preference for *trans* X−Pro substrates is consistent with the ability of pepsin to cleave amide bonds, which are essentially always in a *trans* conformation. Further, it is unclear whether, even if the *cis* peptide were to bind, the arrangement of functional groups in the active site could catalyze the hydrolytic reaction. Hence the experimental observations taken together with the known structure of the binding site (Abad-Zapatero et al., 1990) and the ability of the enzyme to cleave *trans* amide bonds suggest that the isomeric selectivity for X−Pro bond cleavage approaches complete specificity for the *trans* isomer. Of course, analogous to the results for other proteases, it is probable that pepsin cleavage of amide bonds located near an imide X−Pro bond sequence will also exhibit considerable, although perhaps incomplete, conformational selectivity. Such remote partial conformational selectivity has been reported in studies of chymotrypsin and trypsin (Fischer et al., 1984; Lin & Brandts, 1985).

Chart 1

	P_4 P_3 P_2 P_1 P_1' P_2' P_3' P_4'
Ribonuclease A	Ser-Ser-Lys-Tyr-↓-Pro-Asn-Cys-Ala
gag p17/24	Ser-Gln-Asn-Tyr-↓-Pro-Ile-Val-Gln
Avian sarcoma	Thr-Phe-Gln-Ala-Phe-↓-Pro-Leu-Arg-Glu-Ala-OH
Human basic FGF	Ile-Thr-Thr-Leu-↓-Pro-Ala-Leu-Pro-Glu

In the present study, fluorinated analogs of two viral protease substrates reported to be hydrolyzed by pepsin have been investigated: Ser-Gln-Asn-FPhe-Pro-Ile-Val-Gln (FP-1), a substrate corresponding to the gag pl7/p24 junction of the viral gag-pol polyprotein, in which the tyrosine hydroxyl group has been replaced by a fluorine, and Thr-Phe-Gln-Ala-FPhe-Pro-Leu-Arg-Glu-Ala (FP-2), a substrate of avian sarcoma/leukemia virus protease in which the *para* hydrogen on the Phe residue at the P_1 position has been replaced with a fluorine. In order to unmask the conformational preferences of the peptic cleavage, it is necessary to kinetically separate hydrolysis and bond isomerization processes by selecting conditions which increase the rate of the former and minimize the rate of the latter. In view of previous studies indicating that peptide 1 is a poor substrate for pepsin-like enzymes (Copeland et al., 1990), it seemed unlikely that this could be achieved. In fact, conditions were found in which a clear separation occurs, so that the *trans* preference of the enzyme is readily apparent. This may in part reflect the low pH value (2.0) at which the previous assay was performed. Although the digestion of intact proteins such as hemoglobin or albumin by pepsin is optimal at this pH, digestion of the denatured proteins has a pH optimum of about 3.5 (Fruton, 1987; Schlamowitz & Peterson, 1959). In contrast, the avian sarcoma peptide was hydrolyzed too slowly to allow conformational specificity to be determined.

A sequence comparison of the peptides susceptible to X−Pro cleavage by pepsin is given in Chart 1. On the basis of this limited comparison, it appears that optimal substrates for cleavage of the X−Pro bond possess large, hydrophobic residues at P_1, neutral, hydrophilic residues at P_2 and P_3, and residues with aliphatic side chains at P_2' and P_3'. The avian sarcoma peptide, which possesses an Arg at P_3', was found to be a considerably poorer pepsin substrate. Further, the ^{19}F shift of one of the product peptides obtained using FP-2 indicates that although the FPhe−Pro bond represents the primary cleavage site, there is also some initial cleavage at

the Ala−FPhe bond, resulting in a peptide product with N-terminal FPhe. One explanation for this result is that the Arg residue at the P_3' position does not fit well into the corresponding S_3' site, preferring instead an S_4' site, so that the alignment of the substrate in the pepsin binding site is altered. These conclusions are generally consistent with the broader conclusions which have been reached regarding pepsin substrate selectivity (Keil, 1992); there is a general preference for aromatic residues in both P_1 and P_1', and a strong negative effect of Pro in P_1 and Arg in P_3, although no negative effect of Arg at P_3' is reported. Of course, as has been emphasized in studies of HIV protease, the hydrolysis rates of substrate peptides appear to depend not only on the interactions of the substrate side chains with the protease but with each other as well (Ridky et al., 1996). In general, we can conclude from these studies that pepsin is a better model for HIV protease than for avian sarcoma/leukemia virus protease.

As noted recently in our studies of HIV protease (Vance et al., 1997), the requirement of the enzyme for a specific, *trans* peptide bond conformation introduces a slower kinetic time constant into the hydrolysis process, resulting from the need for peptides initially in the *cis* conformation to isomerize. In contrast with the case of HIV protease, this relatively slow process would not present the organism with a significant problem given the stability of pepsin and its role as a digestive enzyme. Hence, there would be no significant need for peptidyl−proline isomerases to enhance the isomerization process.

ACKNOWLEDGMENT

Technical assistance of Scott Gabel is greatly appreciated.

REFERENCES

Abad-Zapatero, C., Rydel, T. J., & Erickson, J. (1990) *Proteins: Struct., Funct., Genet. 8*, 62−81.

Betbeder, D., Caccia, P., Nitti, G., Bertolero, F., Sarmientos, P., Paul, F., Monsan, P., Cauet, G., & Mazue, G. (1991) *J. Biotechnol. 21*, 83−92.

Copeland, T. D., Wondrak, E. M., Tozser, J., Roberts, M. M., & Oroszlan, S. (1990) *Biochem. Biophys. Res. Commun. 169*, 310−314.

Darke, P. L., Chih-Tai, L., Davis, L. J., Heimbach, J. C., Diehl, R. E., Hill, W. S., Dixon, R. A. F., & Sigal, I. S. (1989) *J. Biol. Chem. 264*, 2307−2312.

Fischer, G., Heins, J., & Barth, A. (1983) *Biochim. Biophys. Acta 742*, 452−462.

Fischer, G., Bang, H., Berger, E., & Schellenberger, A. (1984) *Biochim. Biophys. Acta 791*, 87−97.

Fitzgerald, P. M. D., McKeever, B. M., VanMiddlesworth, J. F., Springer, J. P., Heimbach, J. C., Leu, C.-T., Herber, W. K., Dixon, R. A. F., & Darke, P. L. (1990) *J. Biol. Chem. 265*, 14209−14219.

Fruton, J. S. in *Hydrolytic Enzymes* (Neuberger, A., Brocklehurst, K., Eds.) Chap. 1, pp 1−37, Elsevier, Amsterdam, 1987.

Huang, W., & Tang, J. (1969) *Biochemistry 244*, 1085−1091.

Hunkapiller, M. W., & Richards, J. H. (1972) *Biochemistry 11*, 2829−2839.

Keil, B. (1992) *Specificity of Proteolysis*, Springer-Verlag, Berlin.

King, G. F., Middlehurst, C. R., & Kuchel, P. W. (1986) *Biochemistry 25*, 1054−1062.

Kofron, J. L., Kuzmic, P., Kishore, V., Colon-Bonilla, E., & Rich, D. H. (1991) *Biochemistry 30*, 6127−6134.

Kotler, M., Danho, W., Katz, R. A., Leis, J., & Skalka, A. M. (1989) *J. Biol. Chem. 264*, 3428−3435.

Lin, L.-N., & Brandts, J. F. (1979a) *Biochemistry 18*, 43−47.

Lin, L.-N., & Brandts, J. F. (1979b) *Biochemistry 18*, 5037−5042.

Lin, L.-N., & Brandts, J. F (1985) *Biochemistry 24*, 6533−6538.

London, R. E., Davis, D. G., Vavrek, R. J., Stewart, J. M., & Handschumacher, R. E. (1990) *Biochemistry 29*, 10298−10302.

Meek, T. D., Rodriguez, E. J., & Angeles, T. S. (1994) *Methods Enzymol. 241*, 127−156.

Merck Index, 8th ed. (Stecher, P. G., Ed.) p 815, Merck & Co., Rahway, NJ, 1968.

Miller, M., Jaskolski, M., Mohana Rao, J. K., Leis, J., & Wlodawer, A. (1989) *Nature 337*, 576−579.

Moore, M. L., Bryan, W. M., Fakhoury, S. A., Magaard, V. W., Huffman, W. F., Dayton, B. D., Meek, T. D., Hyland, L., Dreyer, G. B., Metcalf, B. W., Strickler, J. E., Gorniak, J. G., & Debouck, C. (1989) *Biochem. Biophys. Res. Commun. 159*, 420−425.

Morris, G. A., & Freeman, R. (1978) *J. Magn. Reson. 29*, 433−462.

Perrin, C. L., & Engler, R. E. (1990) *J. Magn. Reson. 90*, 363−369.

Richards, A. D., Roberts, R., Dunn, B. M., Graves, M. C., & Kay, J. (1989) *FEBS Lett. 247*, 113−117.

Ridky, T. W., Cameron, C. E., Cameron, J., Leis, J., Copeland, T., Wlodawer, A., Weber, I. T., & Harrison, R. W. (1996) *J. Biol. Chem. 271*, 4709−4717.

Schlamowitz, M., & Peterson, L. U. (1959) *J. Biol. Chem. 234*, 3137−3145.

Seelmeier, S., Schmidt, H., Turk, V., & von der Helm, K. (1988) *Proc. Natl. Acad. Sci. U.S.A. 85*, 6612−6616.

Shaka, A. J., Keeler, J., & Freeman, R. J. (1983) *J. Magn. Reson. 53*, 313−340.

Shaka, A. J., Barker, P. B., & Freeman, R. (1985) *J. Magn. Reson. 64*, 547−552.

Stein, R. L. (1993) *Adv. Protein Chem. 44*, 1−24.

Tomasselli, A. G., Hui, J. O., Sawyer, T. K., Staples, D. J., Bannow, C., Reardon, I. M., Howe, W. J., DeCamp, D. L., Craik, C. S., & Heinrikson, R. L. (1990) *J. Biol. Chem. 265*, 14675−14683.

Vance, J. E., LeBlanc, D. A., & London, R. E. (1997) *J. Biol. Chem. 272*, 15603− 15606.

Vanhoof, G., Goossens, F., De Meester, I., Hendriks, D., & Scharpe, S. (1995) *FASEB J. 9*, 736−744.

Wondrak, E. M., Louis, J. M., & Oroszlan, S. (1991) *FEBS Lett. 280*, 344−346.

BI970918B